8th AIAA/ASME Joint Thermophysics and Heat Transfer Conference
24-26 June 2002, St. Louis, Missouri

AIAA 2002-3227

EHD-ASSISTED CONDENSATION OF REFRIGERANT R-134a ON TUBE BUNDLES

Majid Molki*
Department of Mechanical & Industrial Engineering
Southern Illinois University Edwardsville, Edwardsville, Illinois 62026

Michael M. Ohadi
Department of Mechanical Engineering
University of Maryland, College Park, Maryland 20742

Luciana W. Da Silva
Department of Mechanical Engineering
University of Michigan, Ann Arbor, Michigan 48109

An experimental investigation was performed to study the electrohydrodynamic (EHD) augmentation of external condensation on tube bundles. In this research, EHD was implemented by applying a high voltage to spiral electrodes mounted on condensing tubes. The tube bundle consisted of seven enhanced tubes, housed in a shell-type aluminum test chamber. In all the experiments, the condensation fluid was refrigerant R-134a, and the tubes were cooled internally by water provided by a chiller. Six different tube-electrode configurations were considered and tested. The tests were conducted at the saturation temperature of 30°C, with the heat flux and applied voltage in the range of 10 – 30 kW/m^2 and 0 – 20 kV, respectively. The present technique was able to augment the condensation heat transfer coefficient on the average by 30% at 15 kV, while the corresponding average EHD power consumption was only 0.51%. The minimum and maximum heat transfer augmentations were 15% and 50% at 15 kV, corresponding to 0.14% and 1.46% EHD power consumptions. The condensation tests were supplemented by computer simulation of the electric field for each tube-electrode configuration to gain a better insight.

NOMENCLATURE

A	tube outside surface area, m^2
C_i	constant in the Modified Wilson Plot
C_P	specific heat, J/kgK
D	tube diameter, m
EHD	electrohydrodynamic
h	convective heat transfer coefficient, W/m^{2}K
I	electric current, A
L	tube length, m
LMTD	logarithmic mean temperature difference, °C
Nu	Nusselt number
Pr	Prandtl number
$\dot{Q}$	rate of heat transfer, W
$\dot{Q}_{EHD}$	electric power consumption of the charged electrode, W
q	heat flux, W/m^2
Re	Reynolds number
T	temperature, °C
U	overall heat transfer coefficient, W/m^{2}K
V	voltage, V

Greek symbols

α_{EHD}	EHD power consumption ratio

Subscripts

fd	fully developed
H	heater
i	inside
max	maximum
sat	saturated
w	water

INTRODUCTION

Electrohydrodynamics (EHD) is a bi-disciplinary research area that involves the interaction of electric and flow fields. In the present research, EHD is implemented by applying a high voltage to spiral electrodes mounted on tubes of a condenser. The electric body-force generated by the electric field extracts the liquid from the condensing surface and augments the condensation process by facilitating a closer vapor-surface contact. In this investigation, the tube bundle consists of seven enhanced tubes (i.e., the tubes with miniature surface fins) that are housed in an

* Corresponding author: mmolki@siue.edu

aluminum test chamber to simulate a shell-and-tube condenser.

The EHD-enhanced external condensation on single tubes has been the subject of several investigations[1-3]. The effectiveness of EHD on enhancement of external condensation on single tubes is now well established. Wawzyniak et al.[1] improved the average condensation heat transfer coefficient of R-113 by a factor of 1.54 and 2.24 for smooth and enhanced tubes, respectively. Da Silva et al.[3] experimented with the EHD enhancement of external condensation of R-134a on single commercial enhanced tubes. Their results indicated that the external heat transfer coefficient significantly increases under the effect of electric field. The optimum heat transfer enhancement is nearly 3-fold, with the respective EHD power consumption lower than 1% of the test section heat transfer rate.

Research on single-tube condensation has paved the road and facilitated the implementation of EHD in condensers. A number of researchers have designed and tested the EHD condensers[4-7]. Yamashita et al.[4] performed a test-proof of a 50 kW EHD condenser for C6F14 (perflorohexan) and reported a 6-fold enhancement of condensation heat transfer. In an EHD condenser, Sunada et al.[5] indicated a maximum local heat transfer coefficient of over 9000 W/m^{2}K in CFC-113 and over 11000 W/m^{2}K in HCFC-123. Yabe et al.[6] conducted experiments on an EHD evaporator and condenser, and reported that the evaporation and boiling heat transfer of the mixture of R-123 and R-134a on the inner surface of the tube have been enhanced about 3 times over a wide range of qualities with the application of 7 kV at the electrode distance of 2.5 mm.

As evidenced from the foregoing discussion, and despite its strong practical application, the work on EHD condenser is limited. Moreover, a search of literature indicated basically no work on EHD condensers consisting of enhanced tubes. The purpose of the present work is to show the experimental results for external condensation of R-134a in an EHD condenser consisting of enhanced tubes, leading the way towards the design of an efficient EHD condenser in the future.

EXPERIMENTAL SETUP

Figure 1 shows the experimental setup used for testing the tube bundle. The major components of the setup are the pressurized test chamber, water chiller, flowmeter, heater, variac, high voltage power-supply, temperature controller, and pump. The chamber accommodates the horizontal tube bundle comprised of seven enhanced tubes with each tube equipped with a spiral electrode (Fig. 2). The high-voltage power-supply can provide the voltage to all seven electrodes. A pressure transducer measures the pressure inside the chamber, and thermistors measure the temperature of the refrigerant vapor and liquid. The chiller provides cold water to the seven tubes, and the water flow rate can be measured by the flowmeter. The inlet and outlet water temperatures are also measured by thermistors located in the inlet and outlet headers. The helical heater provides the heat of vaporization to the refrigerant. The entire system is insulated by foam insulation to prevent heat losses/gains with the surroundings. The temperature, pressure, voltage, and current are monitored by a HP data acquisition system (DAS). This system is connected to a computer, which makes it possible to observe the data being recorded during the tests.

The heat generated by the electric heater evaporates the refrigerant. The vapor quality at the heater outlet is kept around 0.8 and is controlled by the pump flow rate. Saturated refrigerant is pumped into the chamber and vapor condenses on the tube. The tubes are maintained at a lower temperature by the flow of cold water provided by a constant-temperature chiller. At steady state, the heat removed by the tube balances the heat generated by the heater. Liquid refrigerant from the chamber is pumped into the heater to be heated and evaporated again.

In all the experiments, the refrigerant was R-134a, and the tubes were cooled internally by water provided by the chiller. As shown in Fig. 3, six different designs of tube-electrode configurations were considered and tested. The tests were conducted at the saturation temperature of 30°C, with the heat flux in the range of 10 – 30 kW/m^2, and the applied voltage in the range of 0 – 20 kV (Table 1).

Table 1 - Parameters used in this study

Configuration Number	A	B	C	D	E	F
Number of enhanced tubes	7	7	7	7	7	7
Number of electrodes	7	6	3	1	1	7
Number of cooling tubes	7	7	7	7	1	1
Water flow rate per tube, gpm	4	4	4	4	4; 27	27
Refrigerant	R-134a					
Saturation Temperature, °C	30					
Heat Flux, kW/m^2	10, 20, 30					

DATA REDUCTION

Rate of condensation heat transfer at the tube wall is determined from,

$$\dot{Q} = V_H \cdot I = \dot{m} \cdot C_P (T_{w,out} - T_{w,in}) \qquad (1)$$

In this equation, V_H is the voltage across the heater, I is the heater current, $\dot{m}$ is the total water mass flow rate, C_P is the water specific heat, $T_{w,in}$ is the water temperature entering the inlet header, and $T_{w,out}$ is the

water temperature exiting the outlet header. At steady state, heat generated by the heater is equal to heat removed by the cooling water. The overall heat transfer coefficient is then defined according to,

$$U = \frac{\dot{Q}}{A \times LMTD} \qquad (2)$$

where U is the overall heat transfer coefficient, A (= 0.1288 m^2, 199.6 $in.^2$) is the outside surface area for the 7 tubes based on the tube nominal diameter (D = 19.05 mm, 0.75 in), and LMTD is the Logarithmic Mean Temperature Difference defined as,

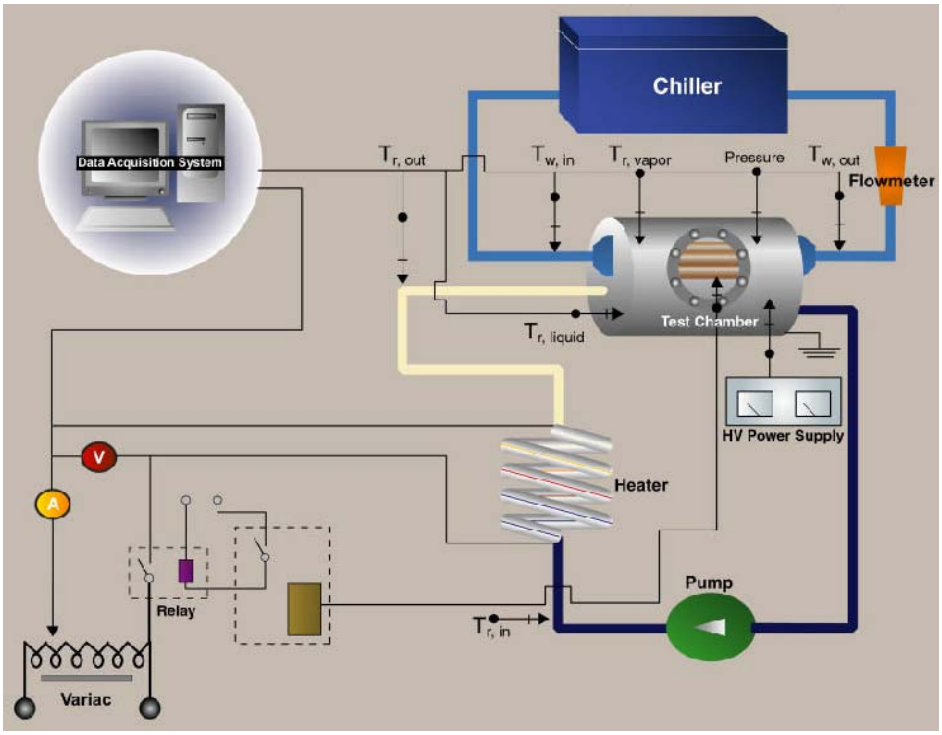

Fig. 1 Experimental setup

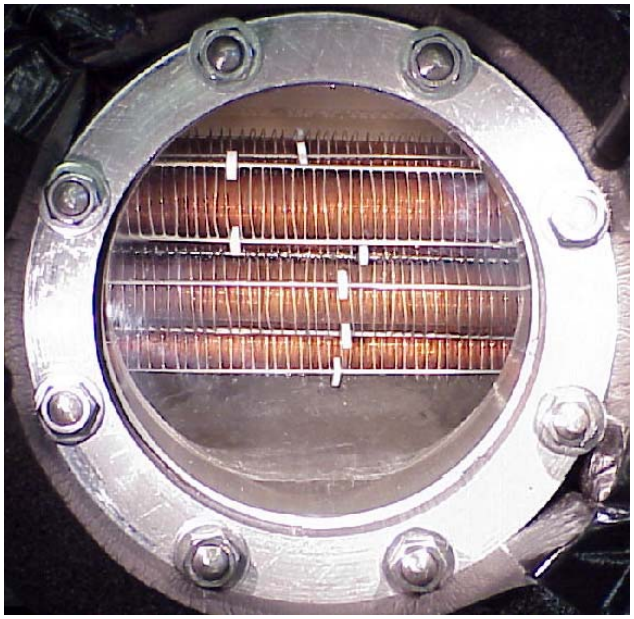

Fig. 2 Tube bundle and electrodes inside the pressurized test chamber

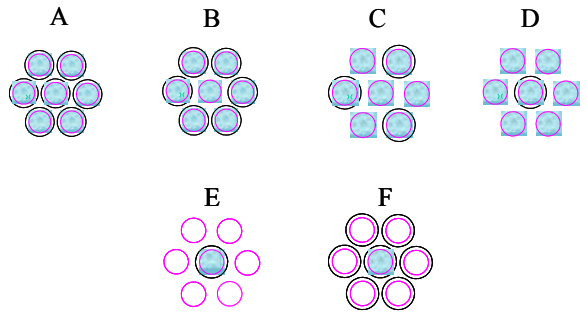

Fig. 3 Electrode positions; Spiral electrode; Gap = 3 mm, pitch = 3 mm

$$LMTD = \frac{(T_{sat} - T_{w,in}) - (T_{sat} - T_{w,out})}{\ln[(T_{sat} - T_{w,in})/(T_{sat} - T_{w,out})]} \quad (3)$$

where T_{sat} is the saturation temperature of the refrigerant.

Note that for configurations E and F, where the cooling water is supplied just to the center tube, external condensation occurs only on that tube and, therefore, the total surface area A = 0.1288 m^2 is divided by 7.

The correlation used for the water-side heat transfer coefficient, h_i, was obtained from the single tube data based on the Modified Wilson Plot[8]. The general form of the Dittus and Boelter[9] correlation is:

$$Nu_{fd} = C_i (0.023)\, Re^{0.8} \cdot Pr^{0.4} \quad (4)$$

where C_i = 2.35 is the parameter obtained experimentally for a single tube. The Reynolds number, Re, is given by

$$Re = \frac{\rho D_{i,max} V}{\mu_w} \quad (5)$$

The heat transfer coefficient predicted by Eq. (4) is corrected for the developing region of the tube according to,

$$\frac{Nu_m}{Nu_{fd}} = 1 + \frac{C}{L/D_{i,max}} \quad (6)$$

where C is a constant and L is the tube length. In this study, C = 2.7 and L = 307.3 mm (12.1 in.). Then, the heat transfer coefficient for the water side, h_i, is obtained from,

$$Nu_m = \frac{h_i D_{i,max}}{k_w} \quad (7)$$

Condensation heat transfer coefficient, h_o, was determined by considering the thermal resistance on the water side, tube wall, and the refrigerant side. Thus,

$$\frac{1}{h_o} = \frac{1}{U} - \frac{D}{D_{i,max} h_i} - \frac{D}{2k} \ln \frac{D}{D_{i,max}} \quad (8)$$

In this equation, k is the thermal conductivity of copper tube wall. For the enhanced tube, k was 310 W/mK. $D_{i,max}$ is the maximum inner diameter of the enhanced tube and is equal to 15.93 mm.

A useful parameter in the EHD condensation is the EHD power consumption ratio. This parameter is defined as,

$$\alpha_{EHD} = \frac{\dot{Q}_{EHD}}{\dot{Q}} \times 100 \quad (9)$$

where $\dot{Q}_{EHD}$ is the electric power consumption of the electrode, and $\dot{Q}$ is the rate of condensation heat transfer defined earlier.

Table 2a – Experimental uncertainty (%) for A

T_{sat} = 30°C				
q [kW/m²]	**0 kV**	**5 kV**	**10 kV**	**15 kV**
10	18	20	25	27
20	16	18	21	22
30	14	17	19	20

Table 2b – Experimental uncertainty (%) for B

T_{sat} = 30°C				
q [kW/m²]	**0 kV**	**5 kV**	**10 kV**	**15 kV**
10	20	22	25	28
20	17	20	21	23
30	16	18	20	22

Table 2c – Experimental uncertainty (%) for C

T_{sat} = 30°C				
q [kW/m²]	**0 kV**	**5 kV**	**10 kV**	**15 kV**
10	17	18	19	20
20	15	16	18	18
30	17	18	19	-

Table 2d – Experimental uncertainty (%) for D

T_{sat} = 30°C					
q [kW/m²]	**0 kV**	**5 kV**	**10 kV**	**15 kV**	**20 kV**
10	16	17	17	18	19
20	16	17	18	19	19
30	12	13	14	14	15

EXPERIMENTAL UNCERTAINTY

The experimental uncertainty of the present work was determined from the ASME guidelines on reporting uncertainties in experimental measurements[10-11]. The precision error, P_h, for each measured parameter, based on 95% confidence interval, is estimated as

- Tube nominal diameter: ± 0.2 mm
- Tube inner diameter: ± 0.2 mm
- Tube length: ± 2 mm
- Voltage: ± 0.1 V
- Current: ± 0.05 A
- Water flow rate: ± 0.00005 m^3/s
- Temperature: 0.1°C

The bias error, B_h, for various parameters was considered negligible. The theory of propagation of uncertainty was applied to evaluate the errors in the final results. The total uncertainty in the final results was calculated as $\Delta_h = \sqrt{P_h^2 + B_h^2}$. Experimental uncertainties are shown in Tables 2a-d. As seen in the table, the uncertainty for the higher values of applied voltage is generally higher. This is due to higher uncertainty of measurements when the condensation heat transfer coefficient is enhanced and the water-side thermal resistance becomes dominant.

Table 3 Test results for bundles A to D, T_{sat} = 30°C

	Heat Flux	h_o	Enhancement				EHD Power %			
	kW/m²	kW/m²K	5 kV	10 kV	15 kV	20 kV	5 kV	10 kV	15 kV	20 kV
	10	13474	1.07	1.39	1.50	-	0.03	0.45	1.46	-
A	20	12303	1.17	1.35	1.43	-	0.01	0.24	1.04	-
7 electrodes	30	10895	1.19	1.34	1.42	-	0.01	0.16	0.81	-
	10	14758	1.12	1.25	1.39	-	0.02	0.12	0.61	-
B	20	13443	1.16	1.23	1.35	-	0.01	0.07	0.33	-
6 electrodes	30	12592	1.12	1.22	1.36	-	0.01	0.06	0.33	-
	10	12166	1.09	1.18	1.19	-	0.00	0.06	0.42	-
C	20	11563	1.09	1.17	1.17	-	0.00	0.04	0.34	-
3 electrodes	30	12582	1.07	1.13	-	-	0.00	0.03	-	-
	10	11276	1.06	1.09	1.15	1.19	0.00	0.02	0.14	0.42
D	20	12011	1.10	1.15	1.19	1.20	0.00	0.01	0.10	0.31
1 electrode	30	9155	1.07	1.13	1.18	1.22	0.00	0.01	0.08	0.29

RESULTS AND DISCUSSION

The first set of tests was conducted on the tube bundle with configuration (A). As seen in Fig. 3, configuration (A) consists of 7 tubes and 7 electrodes mounted on each tube. Table 3 presents the heat transfer coefficients for configurations (A)-(D) when no voltage is applied to the electrodes (h_o) as well as the enhancement of heat transfer coefficient for the range of voltage from 5 to 20 kV applied to the electrodes and the corresponding EHD power consumption. Tests were performed at the refrigerant temperature of 30°C and for the heat fluxes ranging from 10 to 30 kW/m^2. Figure 4 presents a plot of data for configuration (A).

When high voltage is applied to the electrodes, the liquid refrigerant is extracted from the tube surface, and the heat transfer coefficient is enhanced. Moreover, the condensate near the tube surface is agitated and highly turbulent due to the electric field. This mechanism creates a convective effect near the tube surface and is considered an additional factor contributing to the heat transfer enhancement. As seen in Table 3 and Fig. 4, the heat transfer coefficient for configuration (A) can increase up to 50% at 15 kV. The corresponding power consumption is 1.46%. Review of the test data indicates that enhancements of 34 % to 39% can be achieved at 10 kV with a reasonable power consumption of less than 0.5%.

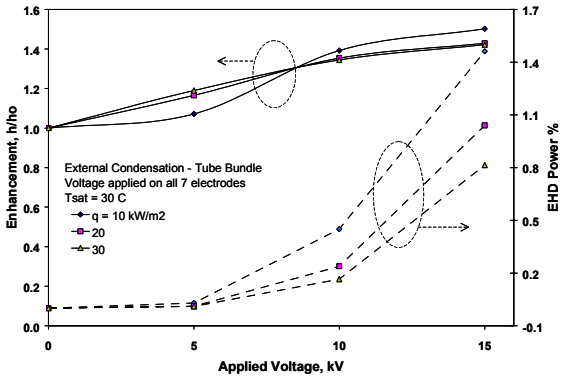

Fig. 4 Test results for configuration A

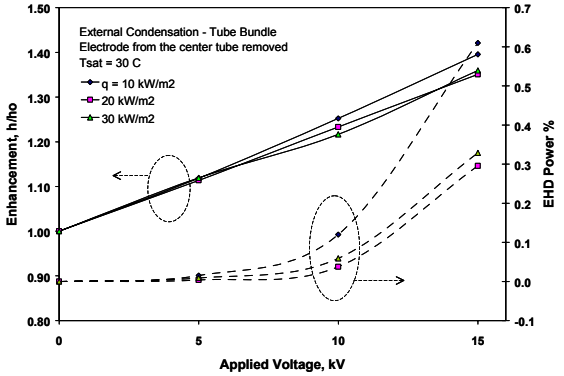

Fig. 5 Test results for configuration B

Test results for configuration (B) are presented in Table 3 and Fig. 5. The difference between this and the previous configuration is that, as seen in Fig. 3, there is no electrode on the central tube in configuration (B).

Review of the data indicates that the base-case heat transfer coefficient (h_o in Table 3) was little affected by removing the central electrode from the bundle, and the difference of 15% between h_o at 30 kW/m^2 for configurations (A) and (B) is within the experimental uncertainty. The enhancement at 15 kV decreased from 1.50 for (A) to 1.39 for (B), but it still represents a considerable enhancement of 39% with the EHD power consumption of 0.61%. Enhancements from 22% to 25% were achieved at 10 kV, with the power consumption lower than 0.12%.

Test results for configuration (C) are shown in Fig. 6. Here, only three of the seven tubes have electrodes and are electrically active (Fig. 3); in other words, the central electrode and three of the external electrodes were removed.

This configuration resulted in the lowest enhancement of heat transfer coefficient for the tube bundle. The three electrodes chosen were able to enhance the heat transfer coefficient by 19% at 15 kV, with a consequent power consumption of 0.42%. Tests at 30 kW/m^2 could not be run for 15 kV due to sparks and refrigerant

breakdown. Moreover, as seen in Fig. 6, beyond 10 kV, the enhancement curves become horizontal. It appears that, beyond 10 kV, the heat transfer coefficients of the charged tubes have reached their peak values and can no longer enhance the overall heat transfer coefficient of the bundle.

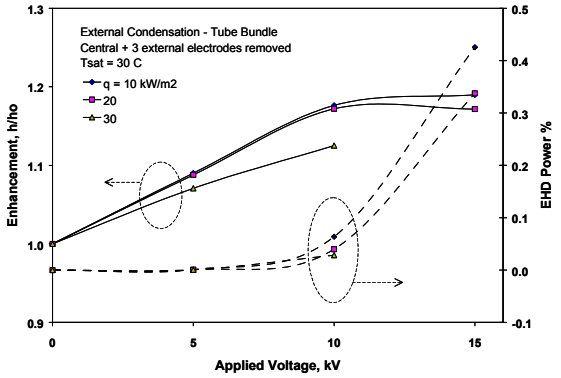

Fig. 6 Test results for configuration C

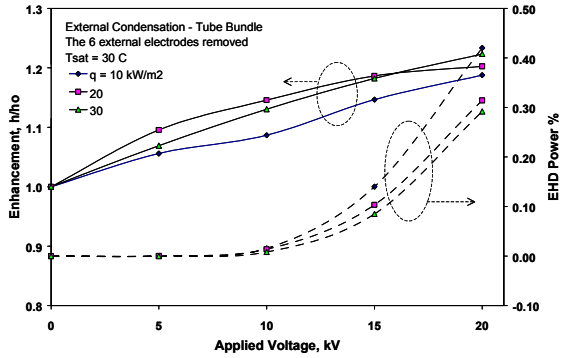

Fig. 7 Test results for configuration D

The test results for configuration (D), where only the central tube of the bundle is equipped with a charged electrode, are presented in Fig. 7. All seven tubes are cooled internally by water and participate in the condensation process. As seen in the figure and Table 3, enhancements of 19% to 22% can be obtained at 20 kV, with the EHD power consumptions of 0.29% to 0.42%. Results of configurations (A) and (D) indicate that the contribution of tubes in heat transfer enhancement is not the same. For example, while the maximum enhancement for seven EHD-active tubes of configuration (A) is 50%, the maximum enhancement for configuration (D) with just one active tube is 22%. It appears that the location of the tubes is an important factor in the EHD-enhanced condensation. The lower tubes are exposed to more condensate than the upper tubes, and it is more difficult to remove the condensate from the lower tubes by the electric body-force. However, the convective and turbulence effects generated by the electric body-force may be more effective on the lower tubes where there is more condensate.

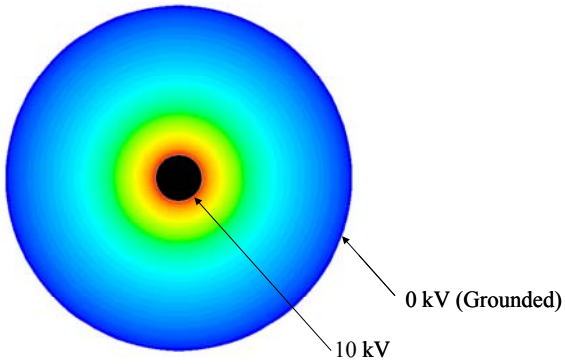

Fig. 8a The potential field is distributed symmetrically around the charged tube.

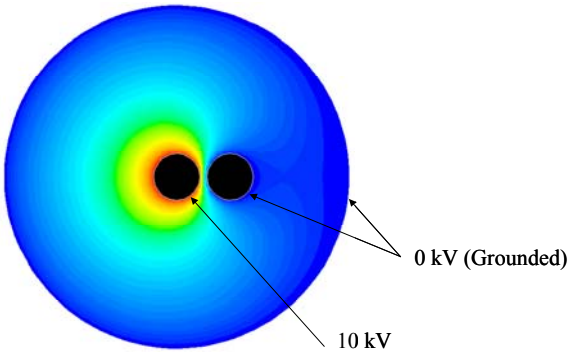

Fig. 8b The potential field is distorted by the presence of the grounded tube.

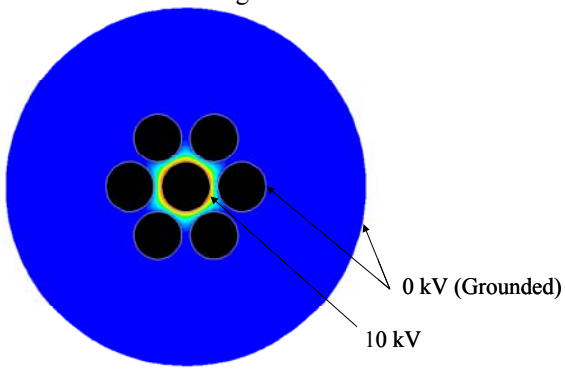

Fig. 8c The grounded tubes block the potential field propagation, allowing a high-potential gradient in the gap between the charged and grounded tubes.

Another noteworthy factor in the EHD-assisted condensation is the nature of the electric field. To gain some insight, we used a simple model for the electric field and obtained the electric field from a numerical solution (Figs. 8a-c). This model is intended to show how the location and number of tubes would affect the electric field. The interaction between the refrigerant

and the electric field was ignored in this model. As seen in the figures, the symmetric electric field of the single tube (Fig. 8a) is distorted in the presence of another tube (Fig. 8b). As additional tubes are introduced in the neighborhood of the central tube (Fig. 8c), the intensity of the electric and therefore the electric body-force is increased. This observation may explain why configuration (D) with one EHD-active tube still performs well. Although configuration (D) is subjected to an intense electric field, configurations (A)-(C) do not have this intense field around all their tubes. For example, in configuration (A), all the peripheral tubes are exposed to a lower filed intensity on the external face of the tube bundle, and the field intensity is strong only in the interior side of the peripheral tubes.

In the aforementioned experiments, all the seven tubes were cooled by water. To examine the performance of single tubes in the bundle, tests were also performed with water flowing just in one tube, namely, the central tube of the bundle. This corresponds to configurations (E) and (F), Fig. 3, in which the external tubes do not participate in the condensation process. Tests were conducted at 30°C and 30 kW/m^2 for water flow rate of 27 gpm (used in our earlier single-tube tests) and 4 gpm (used in the tube bundle tests where all seven tubes participated in the condensation process). The results obtained are presented in Table 4.

Table 4 Test results for bundles E and F

	Heat Flux	h_0	Enhancement				EHD Power %			
	kW/m²	kW/m²K	5 kV	10 kV	15 kV	20 kV	5 kV	10 kV	15 kV	20 kV
E 1 electrode	30 (27 gpm)	26216	1.24	1.35	1.66	1.84	0.00	0.02	0.31	1.21
	30 (4 gpm)	25464	1.38	1.51	1.79	1.95	0.00	0.04	0.40	1.18
F 7 electrodes	10	35299	1.43	2.30	2.78	-	0.01	0.21	2.07	-
	20	30722	1.36	1.72	2.29	-	0.01	0.18	1.33	-
	30	26181	1.32	1.53	1.80	-	0.01	0.20	1.36	-

As seen in the table, the base-case heat transfer coefficient (h_o) for a single tube in the middle of the bundle is comparable to the single-tube results (h_0 ~ 27000 kW/m^2) obtained in our previous tests. Moreover, the data show that the water flow rate has little effect on the heat transfer performance. For configuration (E), enhancements of up to 95% can be obtained with an EHD power consumption of 1.21%. The enhancement obtained in our earlier single-tube tests (~ 3 fold at 20 kV) is not achieved in this configuration. It seems that the presence of the dummy tubes around the condensing tube and the resulting electric field distortion is impeding the higher heat transfer coefficients in the center tube.

The last configuration tested, configuration (F), is shown in Fig. 3. The six dummy tubes around the central tube do not participate in the condensation process, but as they all have electrodes, they contribute to the enhancement of heat transfer coefficient of the central tube. Enhancements of as high as 178% in heat transfer coefficient have been measured for this configuration with higher EHD power consumption of 2.07%. Operation at 10 kV limits the EHD power consumption to 0.21% with a noticeable heat transfer enhancement of 130%. The heat transfer enhancements and EHD power consumptions of the tube bundle for configurations (A)-(D) are summarized in Table 5 for easy reference.

Table 5 Summary of enhancement and EHD power for configurations A-D

Configuration	# of Electrodes	Enhancement, %	EHD Power, %
A	7	50	1.5
B	6	39	0.6
C	3	19	0.4
D	1	22	0.3

CONCLUSIONS

This research on EHD-assisted condensation indicated that the highest heat transfer enhancement for a tube bundle occurs when all the tubes have a charged electrode. This arrangement corresponds to configuration (A) with the maximum heat transfer enhancement and EHD power consumption of 50% and 1.46% at 15 kV, respectively. In configuration (D), where only the central tube has electrode, maximum heat transfer enhancement was 22% with the EHD power consumption of 0.29%. The enhancement of configuration (C) is nearly the same as that in configuration (D) but with higher EHD power consumption which is due to higher number of electrodes in (C). Finally, the configuration (B), with one electrode less that (A), has somewhat less heat transfer enhancement (39% compared to 50% in A), but much lower EHD power consumption (0.61% compared to 1.46% in A).

The present work indicated that EHD-assisted condensation enhances the heat transfer coefficient in tube bundles. The level of enhancement, however, depends on a number of factors including the tube bundle and electrode configuration.

REFERENCES

[1]Wawzyniak, M., Motte, E., Seyed-Yagoobi, J., and Lee, K. A., "Experimental Study of Electrohydro-dynamically Augmented Condensation Heat Transfer on Smooth and Enhanced Tubes," *Proceedings of the 1995 ASME International Mechanical Engineering Congress & Exposition*, San Francisco, CA, 95-WA/HT-21, Nov 12-17, 1995.

[2]Cheung, K., Ohadi, M. M., and Dessiatoun, S. V., "EHD-Assisted External Condensation of R-134a on

Smooth Horizontal and Vertical Tubes," *International Journal of Heat and Mass Transfer*, Vol. 42, 1999, pp. 1747-1755.

[3]Da Silva, L. W., Molki, M., and Ohadi, M. M., "Electrohydrodynamic Enhancement of R-134a Condensation on Enhanced Tubes," *Conference Record - IAS Annual Meeting (IEEE Industry Applications Society), 35th IAS Annual Meeting and World Conference on Industrial Applications of Electrical Energy*, Rome, Italy, Oct 8-12, 2000, pp. 757-764.

[4]Yamashita, K., Kumagai, M., Sekita, S., Yabe, A., Taketani, T., and Kikuchi, K., "Heat Transfer Characteristics of an EHD Condenser (Second Report The development of an EHD Condenser)," *Nippon Kikai Gakkai Ronbunshu, B Hen/Transactions of the Japan Society of Mechanical Engineers*, Part B, Vol. 57, No. 537, May 1991, pp. 1727-1733.

[5]Sunada, K., Yabe, A., Taketani, T., and Yoshizawa, Y., "Experimental Study of EHD Pseudo-Dropwise Condensation," *Nippon Kikai Gakkai Ronbunshu, B Hen/Transactions of the Japan Society of Mechanical Engineers*, Part B, Vol. 57, No. 536, April 1991, pp. 1321-1326.

[6]Yabe, A., Takahashi, K., Aono, H., and Maki, H., "Experimental Study of EHD Heat Exchanger for Nonazeotropic Mixtures," *Nippon Kikai Gakkai Ronbunshu, B Hen/Transactions of the Japan Society of Mechanical Engineers*, Part B, Vol. 59, No. 568, Dec 1993, pp. 3959-3966.

[7]Yamashita, K., and Yabe, A., "EHD Enhancement of Falling Film Evaporation Heat Transfer and Durability of EHD Heat Exchanger," *Proceedings of the 1995 ASME/JSME Thermal Engineering Joint Conference*, Part 4 (of 4), Maui, HI, USA, 1995, pp. 253-260.

[8]Chang, Yu-Juei, Hsu, C. T., and Wang, Chi-Chuan, "Single-Tube Performance of Condensation of R-134a on Horizontal Enhanced Tubes," *ASHRAE Transactions*, Vol. 102, 1996, pp. 821-829.

[9]Incropera, F. P., and DeWitt, D. P., *Introduction to Heat Transfer*, 4th ed., Wiley, New York, 2002, p. 459.

[10]Kline, S., and McClintock, F. "Describing Uncertainties in Single-Sample Experiments," *Mechanical Engineering*, Vol. 75, 1953, pp. 3-8.

[11]Moffat, R. J. "Using Uncertainty Analysis in the Planning of an Experiment," *ASME Journal of Fluids Engineering,* Vol. 107, 1985, pp. 173-178.